# Evolution of a Fluctuating Population in a Randomly Switching Environment

Karl Wienand,[1] Erwin Frey,[1] and Mauro Mobilia[2,*]
[1]Arnold Sommerfeld Center for Theoretical Physics, Department of Physics, Ludwig-Maximilians-Universität München, Theresienstrasse 37, 80333 München, Germany
[2]Department of Applied Mathematics, School of Mathematics, University of Leeds, Leeds LS2 9JT, United Kingdom
(Received 16 June 2017; revised manuscript received 1 August 2017; published 11 October 2017)

Environment plays a fundamental role in the competition for resources, and hence in the evolution of populations. Here, we study a well-mixed, finite population consisting of two strains competing for the limited resources provided by an environment that randomly switches between states of abundance and scarcity. Assuming that one strain grows slightly faster than the other, we consider two scenarios—one of pure resource competition, and one in which one strain provides a public good—and investigate how environmental randomness (external noise) *coupled* to demographic (internal) noise determines the population's fixation properties and size distribution. By analytical means and simulations, we show that these coupled sources of noise can significantly enhance the fixation probability of the slower-growing species. We also show that the population size distribution can be unimodal, bimodal, or multimodal and undergoes noise-induced transitions between these regimes when the rate of switching matches the population's growth rate.

DOI: 10.1103/PhysRevLett.119.158301

Natural populations face ever-changing environmental conditions, which influence their evolutionary fate. For instance, the abundance of nutrients, the presence of toxins, or external factors like temperature and *p*H often influence the evolution of species [1,2]. Several mechanisms have been suggested for a population to cope with fluctuating environments, such as phenotypic heterogeneity, bet hedging, and storing the gains realized during good periods [3–7]. The impact of random environmental changes (external noise) on fitness variability has been studied in population genetics, predator-prey systems, as well as in game-theoretic and related models [8–19]. Demographic fluctuations (internal noise), arising in finite populations, are responsible for fixation—when one species takes over the population [20,21], and determine the population's internal composition. Internal noise is stronger in small populations and becomes negligible in large ones. The dynamics of the population composition is often coupled with the evolution of its size [22–26]. This may result in a coupling of environmental and internal noise, with external randomness affecting the population size, which in turn modulates demographic fluctuations. The interdependence of external and internal noise is especially relevant to microbial communities, which can experience sudden, extreme environmental changes [27–31]. These may lead to population bottlenecks: new colonies or biofilms formed from only few individuals, thus prone to fluctuations. This mechanism leads to feedback loops between social interactions and environment, and to population dynamics of great evolutionary relevance [27–29]. For instance, recent experiments on *Pseudomonas fluorescens* showed that the formation and sudden collapse of biofilms promotes the evolution of cooperative behaviors [30,31].

Most studies, however, treat environmental and internal noise independently [8–19]. Moreover, environmental randomness is often modeled with white noise [8,9,16], although the correlation time is finite in realistic settings. Here, we develop an approach to study the coupled effect of environmental and internal noise on the evolution of a two-species population in a stochastic environment: We assume that the carrying capacity randomly switches between two values, following a dichotomous noise [32,33]. A distinctive feature of this model is the coupling of internal and environmental noise (Fig. 1): Demographic fluctuations depend on the population size that varies following the switching environment. We first consider a scenario with pure resource competition, in which the dynamics of the population composition and its size are only linked by demographic fluctuations. Then, we investigate a public good scenario in which interspecies social interactions

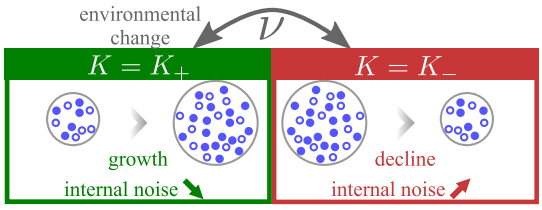


FIG. 1. Cartoon of the model: Coupled evolution of the population size and its composition, consisting of strains $S$ (open circle) and $F$ (filled circle), subject to a stochastically switching carrying capacity $K(t) \in \{K_-, K_+\}$; see Eq. (3). $K$ switches with rate $\nu$ from $K_-$ to $K_+$, leading to population growth and decreasing demographic fluctuations (internal noise). When $K$ switches (with rate $\nu$) from $K_+$ to $K_-$, the population size declines and demographic fluctuations increase.

 

explicitly couple the composition and ecological (size) dynamics. Using analytical and computational means, we show how environmental and internal noise can significantly influence the population's fixation properties. Moreover, we show that external noise induces a transition between different regimes of the population size distribution.

We consider a well-mixed population of finite and time-fluctuating size $N(t) = N_S(t) + N_F(t)$ consisting of two strains. At time $t$, $N_S(t)$ individuals are of a slow-growing strain $S$, corresponding to a fraction $x = N_S/N$ of the population, and $N_F$ are of a fast-growing species $F$. Individuals of strain $\alpha \in \{S, F\}$ reproduce with a per-capita rate $T_\alpha^+ = f_\alpha/\bar{f}$ [23,24], where $f_\alpha$ is the fitness of strain $\alpha$ and $\bar{f} = xf_S + (1-x)f_F$ is the average fitness. Here $f_F = 1$ and $f_S = 1 - s$, where $0 < s \ll 1$ denotes the weak selection intensity that disadvantages the strain $S$ [20]. The population size growth often depends on its composition; e.g., one strain may produce a public good. This is accounted for by multiplying the birth rates $T_\alpha^+$ by a "global fitness" $g(x)$ [22–24]. Here, we focus on two important cases: (i) pure resource competition: $g(x) = 1$, in this setting $x$ and $N$ are only coupled by fluctuations; and (ii) public good: $g(x) = 1 + bx$, corresponding to an explicit coupling of $x$ and $N$, where $x$ represents the fraction of "cooperators" producing a public good and enhances the population growth rate through the benefit $0 < b \sim \mathcal{O}(1)$. Both strains compete for limited resources which constrains the population size as encoded by the death rate $T_\alpha^- = N/K$. We consider that in the presence of environmental randomness, $K$ fluctuates stochastically. The population thus follows a multivariate birth-death process [34,35] in which, at each time increment, an individual at random reproduces [with per-capita rate $g(x)T_\alpha^+$], or dies (with per-capita rate $T_\alpha^-$), or the carrying capacity changes state (with rate $\nu$). The ensuing master equation fully describes the stochastic population dynamics, whose main features are the distribution of $N$ and the probability that $S$ or $F$ fixates by taking over the population, but is difficult to solve [35]. Upon ignoring any form of noise, the population size $N$ and composition $x$ evolve deterministically according to [23,24,36]

$$\dot{N} = N\left(g(x) - \frac{N}{K}\right), \tag{1}$$

$$\dot{x} = -sg(x)\frac{x(1-x)}{1-sx}, \tag{2}$$

where the dot signifies the time derivative. Here, we study the population dynamics subject to a randomly switching carrying capacity (environmental noise) and to stochastic birth and death events (internal noise). We therefore have to account for these sources of noise.

To model environmental randomness, we let the carrying capacity $K(t)$ switch stochastically between a state of abundant resources ($K = K_+$) and one of scarcity ($K = K_- < K_+$). Figure 1 illustrates this stochastic environment and its impact on the population. We consider that environmental switching occurs continuously at rate $\nu$, according to a dichotomous Markov noise $\xi(t) \in \{-1, +1\}$ with zero-mean, $\langle \xi(t) \rangle = 0$ ($\langle \cdot \rangle$ denotes the ensemble average), and autocorrelations $\langle \xi(t)\xi(t') \rangle = \exp(-2\nu|t-t'|)$, where $1/(2\nu)$ is the finite correlation time [32,33]. Hence, the carrying capacity obeys

$$K(t) = \frac{1}{2}[(K_+ + K_-) + \xi(t)(K_+ - K_-)], \tag{3}$$

with average $\langle K \rangle = (K_+ + K_-)/2$. If this is the sole source of noise (no internal noise), the evolution obeys a piecewise deterministic Markov process (PDMP) [18,19,39,40], defined by Eq. (2) and

$$\dot{N} = N\left(g(x) - \frac{N}{\mathcal{K}} + \xi\frac{N(K_+ - \mathcal{K})}{\mathcal{K}K_+}\right), \tag{4}$$

where $\mathcal{K} = 2K_+K_-/(K_+ + K_-)$ is the harmonic mean of $K_+$ and $K_-$. Equation (4) is obtained from Eqs. (1) and (3) as shown in the Supplemental Material [36]. Hence, environmental randomness alone yields a multiplicative noise $\propto \xi(K_+ - K_-)N^2$ in Eq. (4). Demographic fluctuations being ignored, $x$ obeys Eq. (2), which is decoupled from $N$, and evolves on a time scale $\sim 1/s$; see supporting videos [37] and Supplemental Material [36].

Internal noise arises in finite populations when birth and death events occur randomly, and is responsible for fixation. If demographic fluctuations are the only source of noise (say $K$ is constant), the fixation probability $\phi$ of the strain $S$ can be computed from a fitness-dependent Moran process [20,21,41,42] with the same strain-specific fitnesses as in our model, and constant size $N = K$ [43]. Given an initial fraction $x_0$ of $S$ individuals, this probability in a population of constant size $N$ is $\phi(x_0)|_N = (e^{-Ns(1-x_0)} - e^{-Ns})/(1 - e^{-Ns})$ [44,45]. Hence, the fixation probability of the slow strain is exponentially small in large size populations. Since the fixation probability clearly depends on $x_0$, for notational simplicity we henceforth write $\phi \equiv \phi(x_0)$ and $\phi|_N \equiv \phi(x_0)|_N$.

Below, we investigate the *joint* effect of environmental and internal noise on the population dynamics. In particular, since extreme environmental changes can occur more or less rapidly in microbial communities [27–31], we study the influence of the switching rate $\nu$ on the species fixation probability and the distribution of $N$.

*(i) The pure resource competition scenario.*—When $g = 1$, both species simply compete for limited resources. By the competitive exclusion principle [46], $F$ always prevails in the deterministic limit. In this case, the rate equations (1), (2) are decoupled. However, demographic fluctuations, which drive to fixation, scale with the population size: the *stochastic dynamics* of $x$ is thus coupled with that of $N$; see Fig. 1. While $x$ relaxes on a slow time scale

$t \sim 1/s$, $N$ reaches a quasistationary state in a time $t = \mathcal{O}(1)$, see supporting videos [37] and Supplemental Material [36]. Equation (4) is associated with a PDMP whose marginal (unconditioned of $\xi = \pm 1$) stationary probability density function (PDF) is [32,36]

$$p_\nu^*(N) = \frac{\mathcal{Z}_\nu}{N^2}\left[\frac{(K_+ - N)(N - K_-)}{N^2}\right]^{\nu-1}, \qquad (5)$$

where $\mathcal{Z}_\nu$ is the normalization constant and the PDF has support $[K_-, K_+]$. Although this PDF only accounts for environmental noise, it captures the main features of the quasistationary distribution of the population size ($N$-QSD) of the full model when $K_- \gg 1$ [47]. Since $x$ and $N$ evolve on different time scales, the PDF (5) can be combined with $\phi|_N$ to determine the fixation probability. For this, we rescale the switching rate, $\nu \to \nu/s$, to map environmental changes onto the internal dynamics' relaxation time scale, where $\nu/s$ is the average number of switches occurring while $x$ relaxes. Indeed, when $\nu \gg s$ (fast switching), many switches occur prior to fixation and the environmental noise self-averages, whereas when $\nu \ll s$ (slow switching) the population is likely to experience solely the carrying capacity $K_+$ or $K_-$ before one species fixates. The fitness-dependent Moran process gives the fixation probability in those limits. When $\nu \to \infty$, there is self-averaging with $\xi \to \langle\xi\rangle = 0$ in (4) that becomes the logistic equation (1) with $K = \mathcal{K}$, yielding $\phi = \phi|_{\mathcal{K}}$. When $\nu \to 0$, $K$ is equally likely to remain at $K_+$ or $K_-$ until fixation occurs, yielding $\phi = (\phi|_{K_+} + \phi|_{K_-})/2$. Based on these physical considerations, fully detailed in the Supplemental Material [36], we propose to assume the following expression for the $S$ fixation probability when $0 < s \ll 1$ and $K_- \gg 1$:

$$\phi \simeq \int_{K_-}^{K_+}\left(\frac{e^{-Ns(1-x_0)} - e^{-Ns}}{1 - e^{-Ns}}\right)p^*_{\nu/s}(N)dN. \qquad (6)$$

By averaging the effect of internal noise, given by $\phi|_N$, over the external-noise-induced PDF $p^*_{\nu/s}$, Eq. (6) accounts for the fact that $N$ evolves much faster than $x$ relaxes. The expression (6) reproduces the expected results in the two limiting regimes $\nu \gg s$ and $0 < \nu \ll s$. Moreover, Eq. (6) accurately predicts the stochastic simulation results over a broad range of $\nu$ values, capturing the nontrivial $\nu$ dependence of $\phi$, see Fig. 2(a). We find that $\phi$ can increase or decrease with $\nu$ [36] and, importantly, environmental noise can significantly enhance the $S$ fixation probability in *all* regimes: $\phi$ is always greater than $\phi|_{\langle K\rangle}$ obtained in a nonrandom environment with $N = \langle K\rangle$ [36].

We have verified that the mean fixation time scales as $\mathcal{O}(1/s)$ [36]. Hence, after a time $t \gtrsim 1/s$, either species likely fixated and, while the population then only consists of $S$ or $F$, its size keeps fluctuating, see supporting videos [37] and Supplemental Material [36]. Since demographic fluctuations have a marginal influence on the $N$-QSD when $K_- \gg 1$, the PDF $p_\nu^*$ captures its main long-time features;

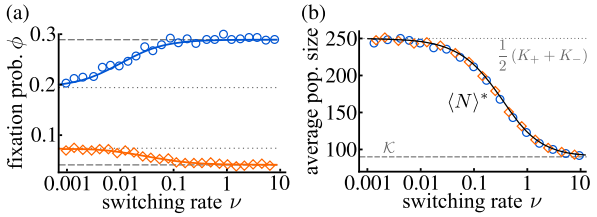


FIG. 2. (a) $\phi$ vs $\nu$ for $(K_+, K_-, x_0) = (450, 50, 1/2)$, with $s = 0.02$ (open circle, blue/black) and $s = 0.07$ (diamond, orange/gray). Symbols are from simulations ($10^4$ runs). Solid lines are from Eq. (6); dashed and dotted lines show $\phi$ when $\nu/s \to \infty$ (dashed) and 0, see text. (b) $\langle N\rangle^*$ vs $\nu$. Symbols are from simulations ($10^4$ runs) with $s = 0.02$ (open circle) and $s = 0.07$ (diamond); they collapse on the curve (solid line) obtained by averaging $N$ over (5); see text.

see Fig. 3. For example, the long-time average population size $\langle N\rangle^*$ is well described by the average over Eq. (5): $\langle N\rangle^* \simeq \int_{K_-}^{K_+} N p_\nu^*(N)dN$, which is independent of $s$ and $x_0$; see Fig. 2(b). The histograms of Fig. 3 show that the environmental noise causes a *noise-induced* transition of the $N$-QSD at about $\nu = 1$ [32]. The transition, predicted by $p_\nu^*$, separates regimes in which environmental change is faster or slower than the population's growth rate. For $\nu > 1$, fast switching results in a unimodal $N$-QSD, see Figs. 3(a), 3(b), whereas for $\nu < 1$, the environment changes slowly and the $N$-QSD is bimodal, see Figs. 3(c), 3(d) and Ref. [36]. The fast decay and slower growth of $N$, characteristic of a logistic dynamics, lead the population size to dwell longer about $K_-$ than about $K_+$. As captured by $p_\nu^*$, this results in right-tailed distributions in Fig. 3. Since Eq. (5) only accounts for external noise, it cannot reproduce some features caused by demographic fluctuations, such as the $N$-QSD not being strictly confined within the support of $p_\nu^*$

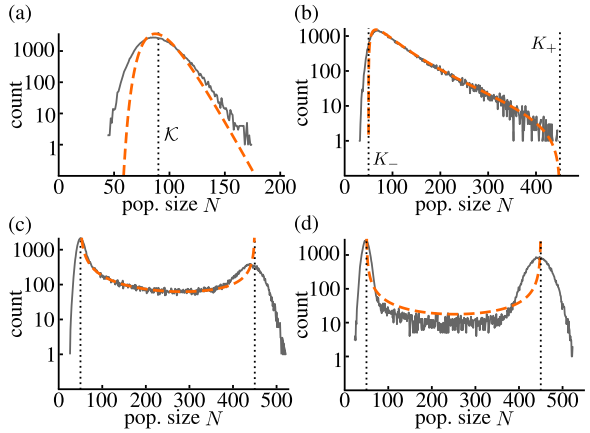


FIG. 3. Histograms of population size ($N$-QSD) and from $p_\nu^*$, for $\nu = 20$ (a), $\nu = 2$ (b), $\nu = 0.2$ (c), and $\nu = 0.02$. (d) Solid lines result from simulations ($10^5$ samples, after $t \gtrsim 1/s$). Dashed lines are the corresponding histograms from Eq. (5). Dotted lines show $N = \mathcal{K}$ in (a), and $N = K_\pm$ in (b)–(d). Parameters are $(K_+, K_-, s, x_0) = (450, 50, 0.02, 0.5)$.

[35,36]. However, as Fig. 2 shows, these deviations only marginally affect $\langle N\rangle^*$ and $\phi$.

*(ii) The public good scenario.*—The above approach can be generalized to cover cases where internal and ecological dynamics are explicitly coupled. As an application, we consider a public good scenario in which $S$ is a "cooperative" strain benefiting the population by enhancing the global fitness $g(x) = 1 + bx$ ($b > 0$) and the carrying capacities, see below. The dynamics of $x$ and $N$ are now coupled, breaking the time scale separation: $N$ becomes a fast variable, enslaved to the slowly varying $x$, see videos 6 and 7 in Ref. [37] and Supplemental Material [36]. After fixation, $x \in \{0, 1\}$ and the $N$-QSD can be obtained as for $b = 0$. When $F$ fixates ($x = 0$), the $N$ distribution is described by $p^*_\nu$ (5). If $S$ fixates ($x = 1$), the population size distribution is captured by $p^*_{\nu,b}$, obtained by substituting $K_\pm \to (1 + b)K_\pm$ and $\nu \to \nu/(1 + b)$ in Eq. (5). Hence, $p^*_\nu$ and $p^*_{\nu,b}$ are the PDFs conditioned to fixation of $F$ and $S$ (but unconditioned of $\xi$), respectively. To address the dynamics before fixation, we approximately account for the correlations between $N$ and $x$ by introducing an effective (constant) parameter $0 \le q \le b$. We then set $g(x) = 1 + q$ in Eq. (4), resulting in a PDMP, decoupled from $x$, for the size of an effective population whose marginal PDF, $p^*_{\nu,q}$ (see Eq. (S2) in [36]), interpolates between $p^*_\nu$ and $p^*_{\nu,b}$. As for $b = 0$, when $0 < s \ll 1$ and $K_- \gg 1$, the $S$ fixation probability in this effective population is [36]

$$\phi_q = \int_{(1+q)K_-}^{(1+q)K_+} \left(\frac{e^{-Ns(1-x_0)} - e^{-Ns}}{1 - e^{-Ns}}\right) p^*_{\nu/s,q}(N)dN. \quad (7)$$

To determine the effective value of $q$ for given $(K_\pm, s, b)$, we consider the limit $\nu \gg 1$, where the environmental noise self-averages, and match the prediction of Eq. (7) with the fixation probability obtained in simulations [36]. As Fig. 4(a) shows, with suitable $q$, Eq. (7) reproduces the simulation results $\phi_q \simeq \phi$ for a broad range of $\nu$ and different values of $b$.

After $t \gtrsim 1/s$, fixation has typically occurred and the population size distributions (when $K_- \gg 1$) are well described by $p^*_{\nu,b}$ ($S$ fixation) and $p^*_\nu$ ($F$ fixation). With these conditional PDFs and $\phi_q$, the long-time average population size reads

$$\langle N\rangle^* \simeq \phi_q \int_{(1+b)K_-}^{(1+b)K_+} N p^*_{\nu,b}(N)dN + \tilde{\phi}_q \int_{K_-}^{K_+} N p^*_\nu(N)dN, \quad (8)$$

with $\tilde{\phi}_q = 1 - \phi_q$. Figure 4(b) shows that Eq. (8) agrees well with simulation results, but cannot capture the behavior at very low $\nu$ ($\phi_q$ being inferred at $\nu \gg 1$). The conditional $N$-QSD and conditional PDFs $p^*_\nu$ and $p^*_{\nu,b}$ present unimodal and bimodal regimes. Specifically, after $S$ fixation, $N$'s growth rate is $1 + b$ and the associated PDF $p^*_{\nu,b}$ undergoes a noise-induced transition at $\nu = 1 + b$.

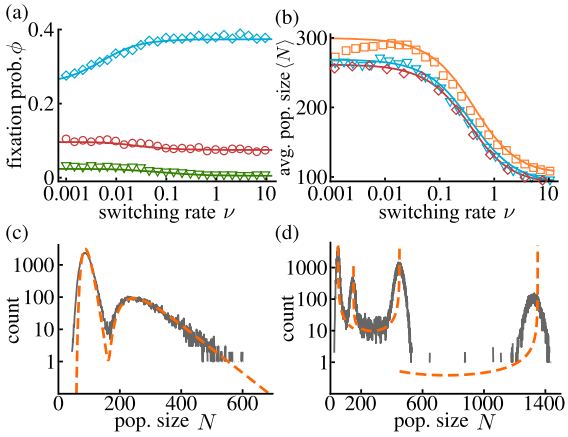


FIG. 4. (a) $\phi$ vs $\nu$ for $(s, b) = (0.01, 0.2)$ (diamond, blue/gray), (0.05,0.2)(open circle, red/black), (0.05,2)(downward triangle, green/dark gray). Solid lines are from Eq. (7). In all panels $(K_+, K_-, x_0) = (450, 50, 0.5)$. (b) $\langle N\rangle^*$ vs $\nu$ for $(s, b) = (0.025, 2)$ (square, orange/gray), (0.05,2) (downward triangle, blue/dark gray), (0.025,8) (diamond, red/black). Solid lines are from Eq. (8). (c),(d) Size distributions for $\nu = 20$ (c) and $\nu = 0.02$ (d), with $b = 2$ and $s = 0.02$. Solid and dashed lines are, respectively, histograms from simulations ($10^5$ replicas, after 99% fixation [36]) and obtained from $p^*_{\nu,b}$ and $p^*_\nu$ weighted by $\phi_q$, see text.

Similarly, the $N$'s growth rate when $F$ fixates is 1, and $p^*_\nu$ undergoes a transition at $\nu = 1$. Since the marginal size distribution is the sum of the conditional distributions weighted by the fixation probability, it is characterized by several regimes and transitions. These properties are well captured by combining $p^*_{\nu,b}$ and $p^*_\nu$ weighted by $\phi_q$, as shown in Fig. 4. When $\nu > 1 + b$, the switching rate exceeds the population's growth rate, and both conditional PDFs are unimodal with different peaks, yielding a bimodal marginal distribution; see Fig. 4(c). For $1 < \nu < 1 + b$, $p^*_{\nu,b}$ is bimodal and $p^*_\nu$ is unimodal. When $\nu$ is below the population's growth rate ($\nu < 1$), both conditional PDFs are bimodal. As a result, the marginal size distribution has three peaks when $1 < \nu < 1 + b$ and four peaks when $\nu < 1$; see Fig. 4(d). As for $b = 0$, the influence of demographic fluctuations on the $N$-QSD is to cause slight deviations from the PDF predictions, particularly at low $\nu$ [36].

Motivated by the evolution of microbial communities in volatile environments, we have analyzed the dynamics of a two-species population subject to a randomly switching carrying capacity (dichotomous noise). A distinctive feature of our model is the coupling of the environmental and internal noise: demographic fluctuations depend on the population size, which in turn changes with the varying carrying capacity (environmental noise). By analytical and computational means, we have studied the coupled effect of environmental and internal noise on the population's ecological and fixation properties. Our analytical approach is based on a time scale separation, arising under weak

selection, between the ecological and internal dynamics. We have also combined the properties of suitable stochastic processes governed solely by internal fluctuations on one hand, and only by environmental noise on the other hand. In the case of pure resource competition (no explicit coupling between internal and ecological dynamics), we have determined the population size distribution, characterized by various regimes, and found that the average size decreases with the switching rate. Assuming a suitable expression for the fixation probability and using stochastic simulations, we have investigated how environmental randomness affects the strains' fixation properties and found that it can significantly enhance the fixation probability of the disadvantaged strain. As an application, we have considered a public good scenario in which internal and ecological dynamics are explicitly coupled. We have thus devised an effective theory that has allowed us to probe the effects of environmental switching and public good benefit on the fixation probability and population composition. We have characterized the population size distribution and the noise-induced transitions between their unimodal (fast switching), bimodal, and multimodal forms, arising when the switching rate matches that of the population growth. Our findings show that coupled environmental and demographic noise can significantly influence the population dynamics by greatly affecting its fixation properties and therefore its composition. This is particularly relevant to microbial communities, which often feature connected internal and ecological evolution.

E. F. acknowledges funding by the Deutsche Forschungsgemeinschaft, Priority Programme 1617 "Phenotypic heterogeneity and sociobiology of bacterial populations," Grant No. FR 850/11-1,2, and the German Excellence Initiative via the program "Nanosystems Initiative Munich" (NIM). M. M. is grateful for the support of the Alexander von Humboldt Foundation, Grant No. GBR/1119205 STP, and for the hospitality of the University of Munich.

*M.Mobilia@leeds.ac.uk

[1] C. R. Morley, J. A. Trofymow, D. C. Coleman, and C. Cambardella, Microbiol. Ecol. **9**, 329 (1983).
[2] C. A. Fux, J. W. Costerton, P. S. Stewart, and P. Stoodley, Trends Microbiol. **13**, 34 (2005).
[3] P. L. Chesson and R. R. Warner, Am. Nat. **117**, 923 (1981).
[4] E. Kussell, R. Kishony, N. Q. Balaban, and S. Leibler, Genetics **169**, 1807 (2005).
[5] M. Acer, J. Mettetal, and A. van Oudenaarden, Nat. Genet. **40**, 471 (2008).
[6] H. Beaumont, J. Gallie, C. Kost, G. Ferguson, and P. Rainey, Nature (London) **462**, 90 (2009).
[7] P. Visco, R. J. Allen, S. N. Majumdar, and M. R. Evans, Biophys. J. **98**, 1099 (2010).
[8] R. M. May, *Stability and Complexity in Model Ecosystems* (Princeton University Press, Princeton, NJ, 1973).
[9] S. Karlin and B. Levikson, Theor. Popul. Biol. **6**, 383 (1974).
[10] E. Kussell and S. Leibler, Science **309**, 2075 (2005).
[11] M. Assaf, E. Roberts, Z. Luthey-Schulten, and N. Goldenfeld, Phys. Rev. Lett. **111**, 058102 (2013).
[12] Q. He, M.Mobilia, and U. C. Täuber, Phys. Rev. E **82**, 051909 (2010).
[13] U. Dobramysl and U. C. Täuber, Phys. Rev. Lett. **110**, 048105 (2013).
[14] M. Assaf, M. Mobilia, and E. Roberts, Phys. Rev. Lett. **111**, 238101 (2013).
[15] P. Ashcroft, P. M. Altrock, and T. Galla, J. R. Soc. Interface **11**, 20140663 (2014).
[16] A. Melbinger and M. Vergassola, Sci. Rep. **5**, 15211 (2015).
[17] M. Danino, N. M. Shnerb, S. Azaele, W. E. Kunin, and D. A. Kessler, J. Theor. Biol. **409**, 155 (2016).
[18] P. G. Hufton, Y. T. Lin, T. Galla, and A. J. McKane, Phys. Rev. E **93**, 052119 (2016).
[19] J. Hidalgo, S. Suweis, and A. Maritan, J. Theor. Biol. **413**, 1 (2017).
[20] J. F. Crow and M. Kimura, *An Introduction to Population Genetics Theory* (Blackburn Press, New Jersey, 2009).
[21] W. J. Ewens, *Mathematical Population Genetics* (Springer, New York, 2004).
[22] J. Roughgarden, *Theory of Population Genetics and Evolutionary Ecology: An Introduction* (Macmillan, New York, 1979).
[23] A. Melbinger, J. Cremer, and E. Frey, Phys. Rev. Lett. **105**, 178101 (2010).
[24] J. Cremer, A. Melbinger, and E. Frey, Phys. Rev. E **84**, 051921 (2011).
[25] A. Melbinger, J. Cremer, and E. Frey, J. R. Soc. Interface **12**, 20150171 (2015).
[26] J. S. Chuang, O. Rivoire, and S. Leibler, Science **323**, 272 (2009).
[27] L. M. Wahl, P. J. Gerrish, and I. Saika-Voivod, Genetics **162**, 961 (2002).
[28] K. Wienand, M. Lechner, F. Becker, H. Jung, and E. Frey, PLoS One **10**, e0134300 (2015).
[29] Z. Patwas and L. M. Wahl, Evolution **64**, 1166 (2009).
[30] M. A. Brockhurst, A. Buckling, and A. Gardner, Curr. Biol. **17**, 761 (2007).
[31] M. A. Brockhurst, PLoS One **2**, e634 (2007).
[32] W. Horsthemke and R. Lefever, *Noise-Induced Transitions* (Springer, Berlin, 2006).
[33] I. Bena, Int. J. Mod. Phys. B **20**, 2825 (2006).
[34] C. W. Gardiner, *Handbook of Stochastic Methods* (Springer, New York, 2002).
[35] K. Wienand, E. Frey, and M. Mobilia (to be published).
[36] See Supplemental Material at http://link.aps.org/supplemental/10.1103/PhysRevLett.119.158301 for the derivation of Eqs. (1), (2), (4), (6), and (7), mean fixation time results, complements to Figs. 3 and 4, and for the description of the supporting videos of Ref. [37]. The Supplemental Material includes Ref. [38].
[37] K. Wienand, E. Frey, and M. Mobilia, figshare. Supporting videos are electronically available at the following URL: https://doi.org/10.6084/m9.figshare.5082712.
[38] D. T. Gillespie, J. Comput. Phys. **22**, 403 (1976).
[39] K. Kitahara, W. Horsthemke, and R. Lefever, Phys. Lett. **70A**, 377 (1979).

[40] M. H. A. Davis, J. R. Stat. Soc. Ser. B **46**, 353 (1984).
[41] P. A. P. Moran, *The Statistical Processes of Evolutionary Theory* (Clarendon, Oxford, 1962).
[42] T. Antal and I. Scheuring, Bull. Math. Biol. **68**, 1923 (2006).
[43] S. P. Otto and M. C. Whitlock, Genetics **146**, 723 (1997).
[44] R. A. Blythe and A. J. McKane, J. Stat. Mech. (2007) P07018.
[45] J. Cremer, T. Reichenbach, and E. Frey, New J. Phys. **11**, 093029 (2009).
[46] G. Hardin, Science **131**, 1292 (1960).
[47] A finite population unavoidably collapses into $(N,x)=(0,0)$. This phenomenon, unobservable when $K_- \gg 1$, occurs after lingering in a quasistationary state well described by the $N$-QSD and $p^*_\nu$.